

CHAPTER 3

METHODOLOGY

3.1 Data Collection

The information of the study areas was collected for this study as follows.

3.1.1 Meteorological data of Bangkok in 1988-1997 were obtained from the Department of Meteorology.

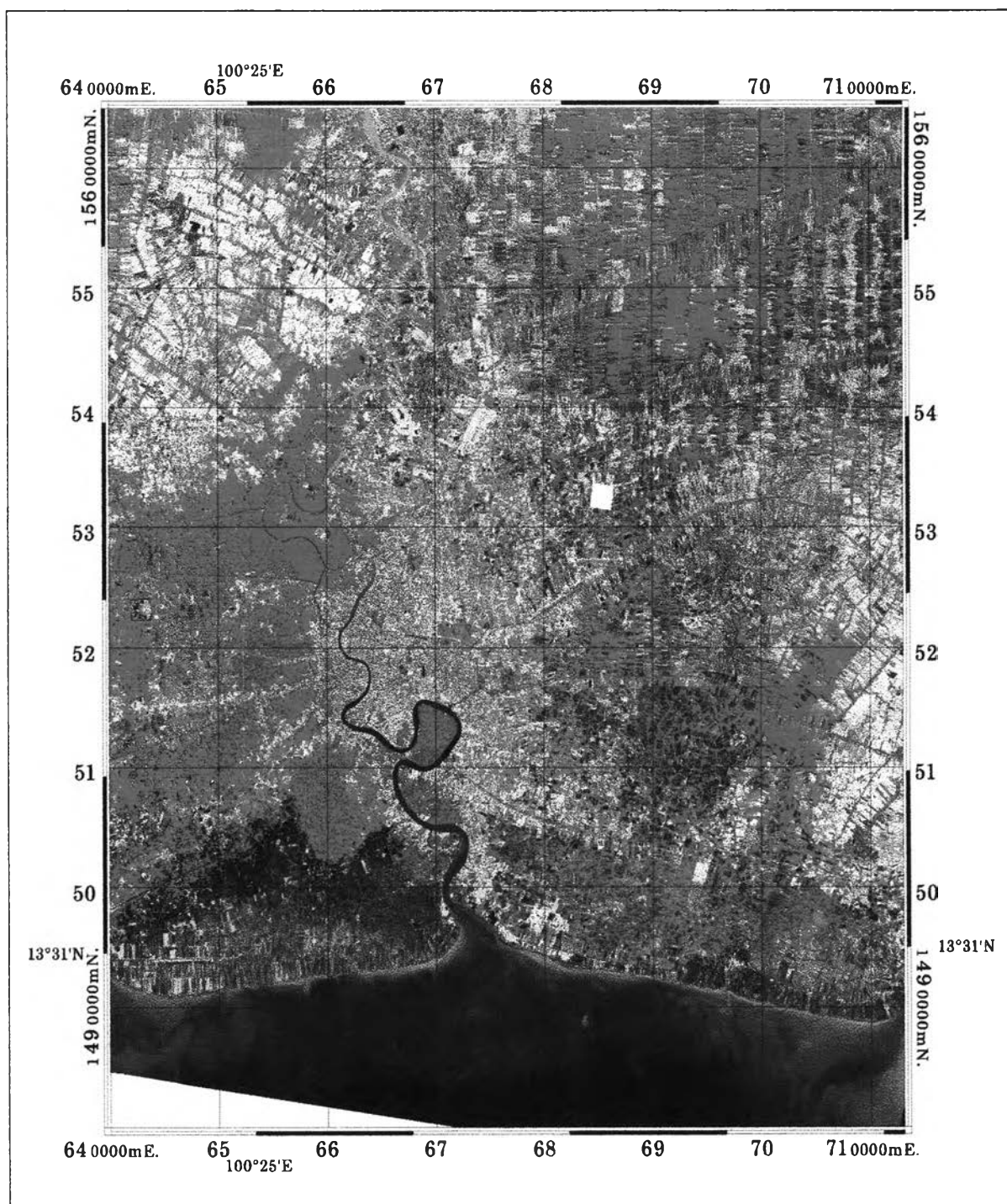
3.1.2 Spatial digital data of Bangkok and vicinities in 1993 were obtained from the Pollution Control Department. They consisted of political boundary, transportation, stream and land use layers.

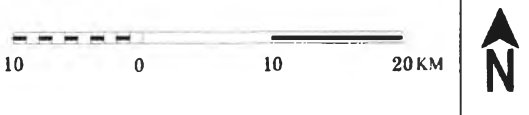
3.1.3 Topographic map at a scale of 1: 50,000, which prepared and published by the Royal Thai Survey Department. Map sheets number 5036I, 5036II, 5037I, 5136I, 5136II, 5136III, 5136IV, 5137II, 5137III, 5236III and 5236IV in L7017 series covered all the study areas.

3.1.4 Survey data of the study areas

3.1.5 Satellite Data set

Radiometrically corrected and geocoded Landsat-5 Thematic Mapper obtained from the National Research Council of Thailand (NRCT). They were acquired on 30 March 1988 and 24 April 1997 with the local time of overpass at 10.40 A.M. Images were subsetted to bounded by rectangle having the upper left corner at 640000E, 1565000N and the lower right corner at 713000E, 1480000N. This covered 6205 square kilometers that represented both urban and non-urban cover types. Plate 2 and 3 show the color composite Landsat TM images, which acquired on 30 March 1988 and 24 April 1997 respectively



<p>PLATE 2: COLOR COMPOSITE LANDSAT TM IMAGE SHOWING BANGKOK METROPOLIS AND VICINITIES ON 30 MARCH 1988</p>	<p>THE EFFECTS OF LAND COVER ON URBAN HEAT ISLANDS IN BANGKOK METROPOLIS</p>
<p>SOURCE : LANDSAT TM (bands 4, 3, and 2 : RGB) ACQUIRED ON 30 MARCH 1988</p>	

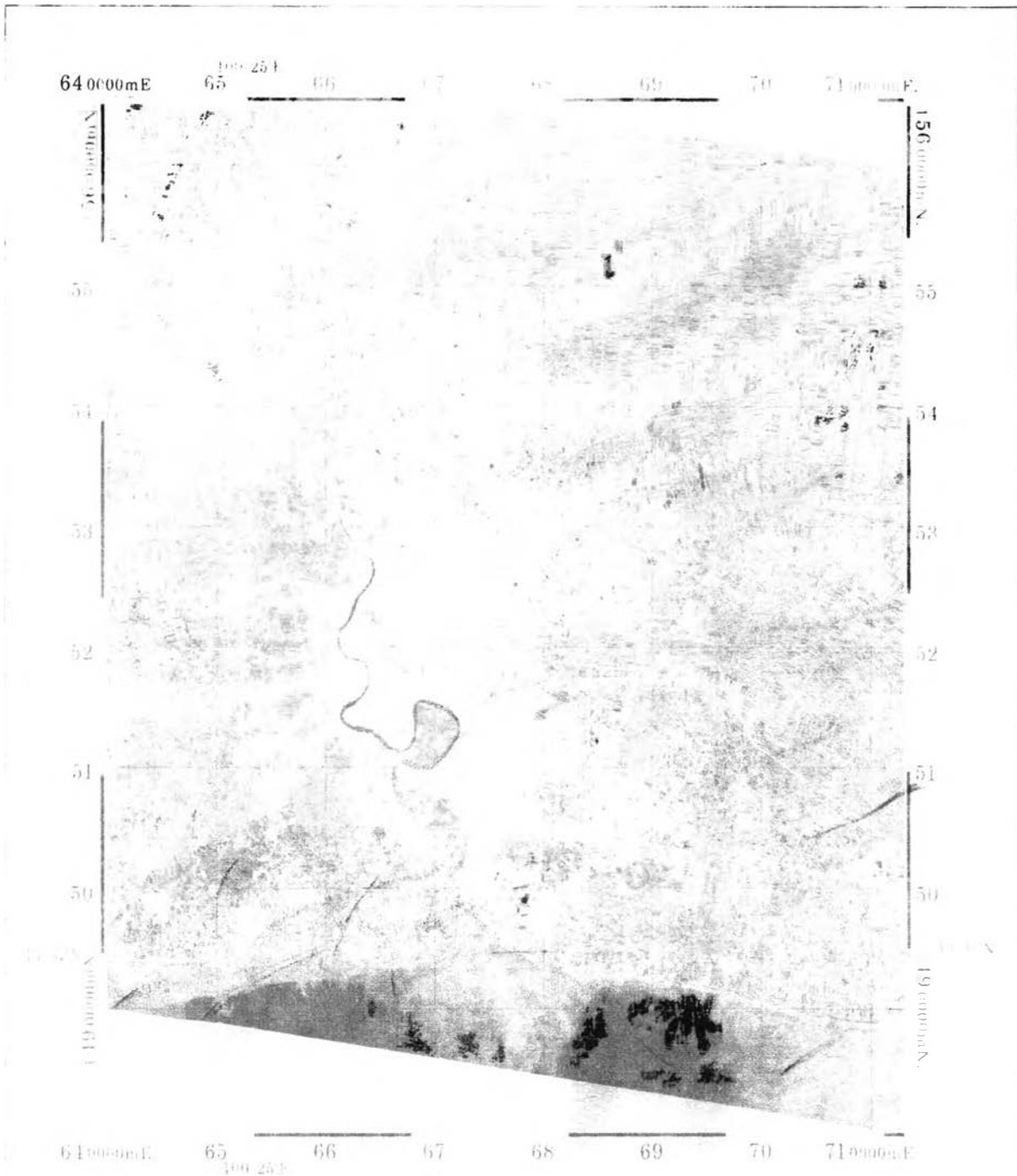


FIGURE 1. COLOR COMPOSITE LANDSAT IMAGE SHOWING BANGKOK METROPOLIS AND SURROUNDING AREAS ACQUIRED ON 24 APRIL 1997.

SOURCE: LANDSAT IMAGERY (Landsat 7, and TM RGB) ACQUIRED ON 24 APRIL 1997.

FIGURE 2. THE EFFECTS OF LAND COVER ON URBAN HEAT ISLANDS IN BANGKOK METROPOLIS.



3.2 Materials and Equipment

3.2.1 A personal computer with format tape drive for reading satellite data, super VGA graphic card and monitor

3.2.2 Software

3.2.2.1 PCI program version 6.1 for satellite data processing and analysis (PCI, 1997)

3.2.2.2 ARC/INFO program version 3.4.2 for spatial information preparation (Environmental Systems Research Institute [ESRI], 1990)

3.2.2.3 Adobe Photoshop version 4.0 for data presentation (Adobe, 1996)

3.2.3 Global positioning system (GPS)

3.3 Methodology

Satellite data of the two dates were processed to derive TVI, land use / land cover type and surface radiant temperature. Then, these data were considered with the ancillary data for image interpretation. Finally, evaluated the relationship between surface radiant temperature, TVI on patterns of land cover type. Work flow diagram is shown in Plate 4.

This study proceeded through the following steps.

3.3.1 *Pre-processing*

- Image rectification and restoration

The image rectification procedure was considered as pre-processing for quality of image improving before image analysis step.

The Geometric Correction processing used topographic map at a scale of 1:50,000 as the reference data for geometric correction. The procedure can be described as follows

Ground Control Points (GCPs) were collected from satellite image in line and pixel coordinate, then specified in UTM coordinate, which obtained from topographic map at the

and on the satellite image and also do not change through time being used. Road intersections and bridges were selected as GCPs in this study.

The UTM coordinate of each GCPs in the corrected matrix are transformed to determine their corresponding location in the original distorted image.

Nearest Neighborhood technique, which transfer grey level of the nearest pixel were used in resampling procedure to interpolate grey levels from pixel locations in the original distorted image and their relocation to the appropriate matrix coordinate location in the rectified image.

- Image Enhancement

Linear Stretch technique (Figure 9) was used to enhance image in order to improve the visual interpretability of an image. Image pixels with close grey level values may now be displayed in sufficiently different grey tones distinguished.

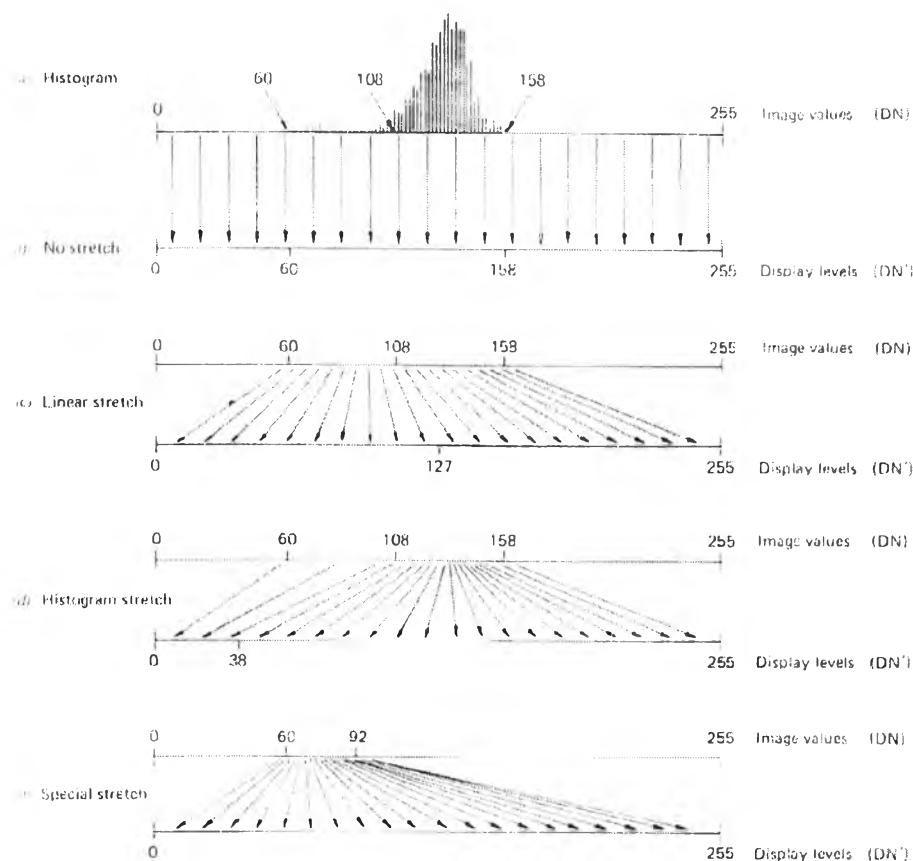


Figure 9: Principle of contrast stretch enhancement (Lillesand and Kiefer, 1994)

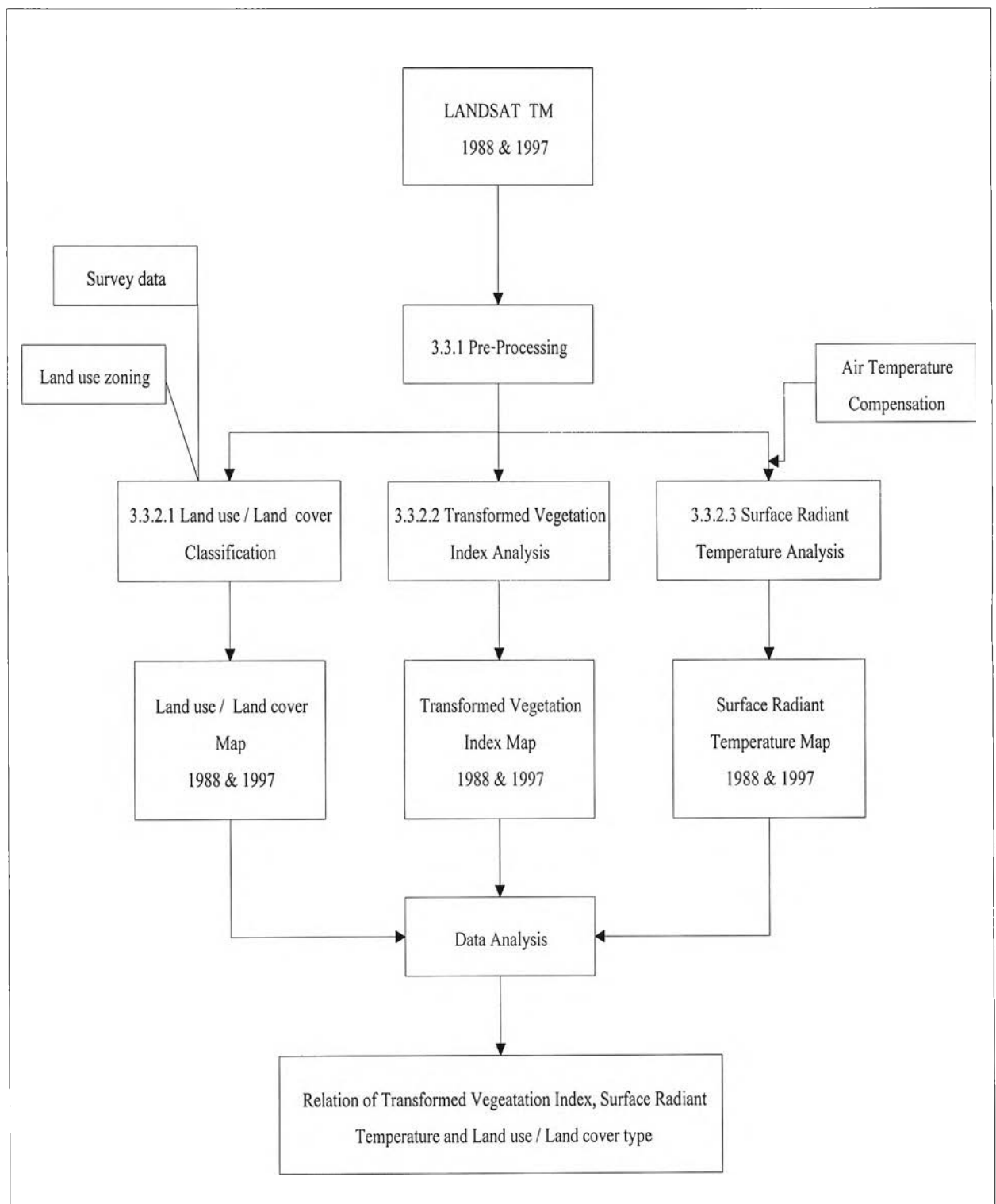


Plate 4: Work flow diagram

3.3.2 Data processing

3.3.2.1 Land use / land cover Classification

All pixels on image were categorized into land use / land cover classes in this stage by supervised classification method.

Image classification made according to the following procedures

(1) Training stage

False color image was displayed for classes identification assistance. The most alike color pixels were grouped to be the representative training areas, and the numerical parameters of the spectral patterns were developed for each land cover type. Because of the several of spectral patterns within each individual class, training sites were determined at sub-class levels for improving image classification efficiency. Then these sub-classes were merge into the major classes after the classification stage based on the most likeliness of spectral patterns.

(2) Classification stage

Maximum Likelihood techniques was used to be the mathematical decision rules to categorize each pixel on the image.

This technique is one of the most popular methods of classification in remote sensing because it produces the higher classification accuracy than the others (Kunya Tisayakorn *et al.*, 1993). Many studies (H.R.H. Princess Maha Chakri Sirindhorn *et al.*, 1989; Forster, 1991; Karale, Radhadrishnan and Chandrasekhar, 1991; Supan Kanjanasuthum, 1993; Harris and Ventura, 1995) used Maximum Likelihood techniques for land use / land cover classification.

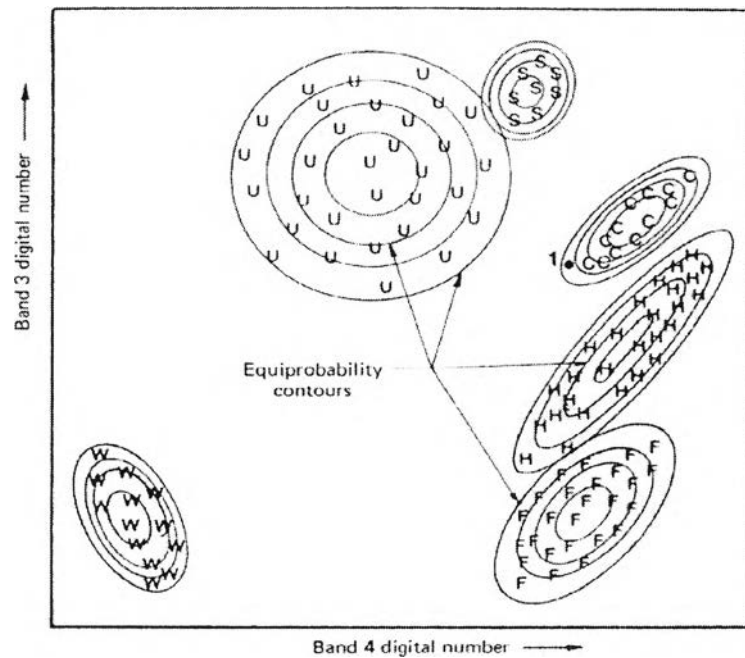


Figure 10: Equiprobability contours defined by a maximum likelihood classifier
(Lillesand and Kiefer, 1994)

Likelihood is defined as the posterior probability of a pixel belonging to any class. The mean vector and covariance matrixes of the category spectral values were considered when classifying an unknown pixel. To do this, an assumption is made that the group of point representative of each category training area is normal distribution. For each cluster, ellipses are drawn about the mean, depending on the distribution of points in the cluster as shown in Figure 10 (Molenaar, 1993; Lillesand and Kiefer, 1994).

Land use / land cover classification using only satellite data can be categorized into seven primary classes. There are built-up area, vegetation area, bare soil, harvested paddy field, marsh land, aqua-culture pond, and water body. Because of the only use of spectral pattern classification and the spatial resolution of Landsat TM were still inadequate for accurate and consistent urban classification (Martin and Howarth, 1989 cited in Harris and Ventura, 1995). Therefore, the GIS data of land use zoning were used as the ancillary data in order to classify built-up area into three secondary classes; residential area, industrial area, and residential and

industrial mixed area. For urban and rural separation, the margin of built-up areas that located at the center of study area was used as the boundary of urban area, and the area out of this boundary was rural area.

This study focused on the land uses and various surface properties of land cover types, which are potentially affecting the heat island. Thus the images were classified into nine land use / land cover type that shown in Table 8.

Table 8 : Land use / land cover type and their definition for the present study

Land use / land cover type	Definition
(1) Residential area	Residence, commercial and offices
(2) Industrial area	The Bang Pu industrial estate as delineated from land use zoning in 1993*
(3) Residential and industrial mixed area	Residential and industrial mixed area*
(4) Vegetation area	Area covered with fully growth vegetation (agricultural area, parks and unused lands)
(5) Bare soil	Open space, cleared paddy field
(6) Harvested paddy field	Harvested paddy field still covered with rice trash
(7) Growing paddy field or marsh land	Area in paddy field with flooded and wetland
(8) Aqua-culture pond	Aqua-culture ponds
(9) Water body	River, streams, natural ponds

* Remark: Bang Pu industrial estate is delineated to determine the effect of industry park and temperature. Other industrial areas are considered in residential and industrial mixed area.

(3) Output stage

The image classifications were presented in the pseudo-color image. The different colors represented the difference of land use / land cover types in Bangkok Metropolis.

3.3.2.2 Transformed Vegetation Index

The vegetation indexes of two date's image were computed in the terms of Transformed Vegetation Index (TVI) percentage. It can be expressed as

$$\% \text{ TVI} = \left[\left[\frac{\text{IR} - \text{Red}}{\text{IR} + \text{Red}} + 0.5 \right]^{\frac{1}{2}} * 100 \dots \dots \dots (1) \right]$$

where IR and red band correspond to the digital number in bands TM4 and TM3, respectively.

The outputs of vegetation covering rate of the study area were presented in the pseudo-color image. The different color tones represented the variation of vegetation density.

3.3.2.3 Surface radiant temperature Analysis

The surface radiant temperature for this study were derived from Landsat TM band 6 (10.4 – 12.5 μm). Equations developed by the National Aeronautics and Space Administration (NASA) were used to transform raw satellite data into absolute radiance and temperature values consequently.

Firstly, the digital numbers were converted to blackbody equivalent radiance values.

$$L(\lambda) = L_{\min}(\lambda) + \frac{[L_{\max}(\lambda) - L_{\min}(\lambda)] * Q_{\text{cal}}}{Q_{\text{cal max}}} \dots \dots \dots (2)$$

where $L(\lambda)$ = the radiance received by the sensor
 $L_{\min}(\lambda)$ = the minimum detected radiance for the sensor
 $L_{\max}(\lambda)$ = the maximum detected radiance for the sensor
 $Q_{\text{cal max}}$ = the maximum grey level (255)
 and Q_{cal} = the grey level or digital number for each analyzed pixel

Then the radiance values can be converted into surface radiant temperature by reverse analysis of the Planck's equation.

$$T(K) = \frac{K_2}{\text{Ln} [(K_1 + 1) / L(\lambda)]} \dots\dots\dots(3)$$

where $T(K)$ = apparent temperature (also known as brightness temperature or radiant temperature)

K_1 = the calibration constant

and K_2 = the calibration constant

NASA supplies the sensor calibration data as follows.

$$L_{\min}(\lambda) = 0.1238 \text{ mW.cm}^2.\text{sr}^{-1} . \mu\text{m}^{-1}$$

$$L_{\max}(\lambda) = 1.56\text{mW.cm}^2.\text{sr}^{-1} . \mu\text{m}^{-1}$$

$$K_1 = 60.766 \text{ mW.cm}^2.\text{sr}^{-1} . \mu\text{m}^{-1}$$

$$\text{and } K_2 = 1260.56 \text{ K}$$

These equations assume that the Earth-atmosphere interface behaves as a black body, and that the calibration constants are time independent. This transformation procedure was widely used for temperature study. (Schott and Volchok, 1985; Markham and Barker, 1986, cited in Desjardins, Gray and Bonn, 1990; Smith and Choudhury, 1990).

Because this study is interested in relative temperature of land use / land cover type by assuming the atmospheric effects are spatially uniform, thus the atmospheric correction have not been carried out. But the air temperature of Bangkok, observed by the Department of Meteorology, on the day of satellite overpass, were used to compensate the two images in order to minimize the atmospheric effect. This was done by modifying equation (2) to:

$$L(\lambda) = \frac{L_{\min}(\lambda) + [L_{\max}(\lambda) - L_{\min}(\lambda)] * (Q_{\text{cal}} + Q_{\text{compensate}})}{Q_{\text{cal max}}} \dots\dots\dots(4)$$

where $Q_{\text{compensate}} = \left[\frac{L(\lambda) - L_{\min}(\lambda) * Q_{\text{cal max}}}{[L_{\max}(\lambda) - L_{\min}(\lambda)]} \right] - Q_{\text{cal}}$

$$L(\lambda) = e^{(\ln(K1+1) - k2/T)}$$

The thermal images were presented in pseudo-color image. The different color tones represented the variation of temperature's magnitude.